Mechanical impedance reveals the decoupling caused by partial squeeze-film levitation

Nicolas Huloux, Corentin Bernard, and Michaël Wiertlewski *Member, IEEE*

Abstract—Friction-modulation can produce tactile sensations directly on bare fingertips interacting with touchscreens. Ultrasonic squeeze-film levitation is one of the methods to significantly modulate the frictional resistance. As transverse ultrasonic vibrations propagate through a plate, they are self-demodulated at the contact with the skin, thus reducing friction. Part of the energy provided by the plate is absorbed by the tissues, resulting in a conspicuous change in vibration amplitude which can be used to measure the fingertip impedance. However, the relationship between the amplitude of vibration and the impedance remains unclear. In this study, the dynamic behavior of the plate, the tissues and the contact is modeled at two time-scales; one for the harmonic behavior at ultrasonic frequency which explains the flux of energy and another one for the quasi-static behavior of the contact. The experiment performed confirm that the model accurately describes the influence of the amplitude on the observed impedance (i.e. the amount of energy absorbed and reflected) by the plate-finger system ($R^2 = 0.80 \pm 7$). The results point out that the amount of energy required to sustain the levitation decreases as the amplitude increases. The role of contact dynamics in ultrasonic friction-modulation can contribute to designing energy-efficient devices generating powerful physical sensations.

Index Terms—Ultrasonic friction-modulation, Squeeze-film, Tactile Devices, Surface Haptics, Biomechanics

1 Introduction

In spite of the central role of touch in sensory-motor coordination, current human-computer interfaces often lack any tactile feedback resulting in a clumsy and slow interaction and requiring visual attention. Designers of electronic consumer devices have started to address this lack by developing touchscreens equipped with vibrotactile feedback. Although these devices often provides an improved interaction the rendering is limited to transient signals. A novel class of devices, called surface-haptics, bridge this gap by providing low-frequency tactile stimuli to users interacting with a screen. These stimuli can simulate the sensation of exploring bumps and holes or can guide the user in , directly by modulating the force applied to the fingertip [1], [2], [3], [4], [5], [6], [7].

Friction modulation via ultrasonic near-field levitation is arguably one of the most promising methods to create surface haptics devices. When the skin of a fingertip is in contact with a surface excited with transverse displacement a thin film of air is trapped and non-linearly compressed which results in a squeeze-film levitation of the skin [8]. The over-pressure caused by the squeeze-film reduces the intimate contact area between the skin and the surface, resulting in a lower interfacial friction [9] and a feeling of slipperiness when the ultrasonic vibration is large enough [10].

Part of the acoustic energy stored in the vibration of the plate is converted into the levitation of the skin, creating a gap that increases with the amplitude of vibration. In addition to the levitation, the skin oscillates at the same excitation frequency than the plate. During each oscillation, the gap closes creating a cushion of air on which the tissues bounce [11]. The other notable effect is that the vibration of a plate, driven at a constant harmonic force, is reduced by the presence of an object levitating to which acoustic energy is transferred [12]. An estimation of fingertip mechanical properties around the excitation frequency [13], [14], [15] and even of the value of the levitation force [16] can be found by comparing the complex impedance of the plate with and without the presence of the finger.

Kaci et al. showed that the acoustic force increases linearly for low amplitude of the ultrasonic wave, but reaches an inflection point at higher amplitudes [16]. This result lends itself to the hypothesis that the transmission of acoustic energy from the plate to the finger might be influenced by the amplitude of the stimulation. A positive-feedback loop might exists where higher vibration requires smaller forces for levitation thus leading to larger gap and so on.

We developed a new dynamic model of the squeeze film levitation to explore in further details the coupling between the skin and the ultrasonic plate and its consequence on the transfer of acoustic energy. Contrary to previous models which consider the plate as a pure source of displacement [9] or where the skin firmly attached to the plate [17], this model couples the physics at the interface with the dynamics to paint a more precise representation of the interaction. The simulation correctly predicts the influence of the ultrasonic vibration on the total measured impedance — which informs on the transfer of energy between the various bodies in contact— found by comparing the amplitude and phase of the force produced by the actuators with the actual harmonic motion of the plate. This work renders possible the estimation of the state of the contact and the biomechanics of the skin in real-time, which can be used to optimally drive surface-haptic devices.

- *N. Huloux is with Aix-Marseille Univ., CNRS, ISM, Marseille France*
- *C. Bernard is with the Perception Representation Image Sound and Music laboratory, Aix-Marseille Univ., CNRS, Marseille, France.*
- *M. Wiertlewski is with TU Delft, Delft, The Netherlands. m.wiertlewski@tudelft.nl*

This research was supported by the Agence Nationale de la Recherche project IOTA ANR-16-CE33-0002

2 BACKGROUND

2.1 Friction reduction theories

The first theories of ultrasonic friction-modulation revolved around the principle of squeeze-film levitation [8], [10]. The air is trapped between the vibrating plate and an idealized rigid and flat fingertip. Because of the vibration, the gap between the plate and the finger closes quickly for the air to escape from the edges of contact therefore compressing the latter. This non-linear process creates an net force on the skin. This so-called squeeze-film effect has been extensively studied in the ideal case of two flat surfaces [18] but only recently it has been extended to soft and conformable tissues. An alternative of squeeze-film theory, which did not involve air, argue that the skin is bouncing on the plate, making intermittent contact of short duration resulting into a reduction of the overall friction [19], [20]. However, recent investigations under reduced pressure shows that the air is a critical factor in the modulation of friction [11], [21].

Taking into account the fact that the skin is compliant and rough, a new theory, backed by experimental data, suggests that the mechanism behind the reduction of friction involves both the squeeze-film levitation and bouncing [9]. However, the skin bounces on a film of air and not on the plate, resulting in a interfacial gap that is monotonically growing with increasing amplitude. Both the skin and the plate move creating a dynamic non-linear system. The current article is an attempt at modeling the behavior of the skin bouncing on the plate as well as its effect on the oscillation of the plate.

2.2 Finger mechanics

It has been shown that the mechanical properties of the skin have a significant effect on the friction reduction. Fingertips that are too elastic tend to be unaffected by the ultrasonic vibration [13], [22]. Similarly, fingers that have a large mass and damping also suffer from less variation of friction than others [15]. The mechanical behavior of skin and in particular on the finger has been extensively studied in the low frequency end of the spectrum where it behaves mostly as an over-damped spring and damper system [23], [24], [25], [26] but little is known in the ultrasound range. In order to capture high-frequency behavior some model are composed of a series of mass spring damper in series [27]. Recent measurements leveraging the self-sensing capabilities of the ultrasonic friction-modulation devices, show that in the 30 to 40 kHz range, the skin behaves as a 0.1 ± 0.04 g mass in parallel with a $22 \pm 10\mathrm{N.s.m^{-1}}$ damper [15]. At these frequency the elasticity of the tissues does not contributes any significant forces and therefore can be neglected. Lastly, every single study confirms that the inter-personal variability of the dynamic properties of the skin is considerable and are the most likely reason why the effect of ultrasonic friction-modulation is variable from individual to individual.

2.3 Contact mechanics

The contact between the skin and the plate also influence strongly the process of levitation and therefore the behavior of ultrasonic friction-modulation. In particular, the relationship between the force required to maintain both bodies in contact and the size of the gap is of upmost interest to model the dynamics. The skin is soft and rough and therefore the contact between the plate and the fingertip is not as straightforward as the contact between two flat surfaces. Aside from the gross deformation which closely resemble Hertzian contact theory, the ridges of the skin could be modeled with local Hertzian contact at random height, as per Greenwood and Williamson theory [28]. Instead of considering the interaction at only two spatial scales –the fingertip and the ridges–, multiscale contact theory provides a mathematical framework to model the interaction between two randomly rough surfaces. In this model, the gap for a given force is predicted by the shape of the frequency spectrum of the roughness. The roughness is seen as a fractal, in which Hurst exponent and the size of the asperities height distribution at a level of magnification determines completely the state of the contact between both bodies [29].

2.4 Mechanical Impedance

Ultrasonic friction modulation devices are typically constructed around a circular or rectangular plate actuated at a single ultrasonic frequency via piezoelectric actuators. An AC-voltage is applied to the actuator which results in a harmonic deformation of the plate. The plate and the piezoelectric actuators have reactive elements –mass, spring or capacitance– and dissipating elements –damper, resistors. The amplitude and phase of the motion with respect to the amplitude of the force depends on these parameter. To capture the dynamics of the system, it is useful to introduce the notion of impedance, generalizing the dynamic of the reactive and dissipating lumped-elements, which is a complex value that links the harmonic force to the harmonic velocity.

The real part of the impedance reflects the dissipation of energy through the dissipating elements and the imaginary part, which can be both positive and negative, reflects the reaction of from elements that store energy. Common complex impedance of mass, spring and damper are known and related to their physical parameters, and their impedance for a given angular frequency ω are: $Z \propto i\omega$ for the mass, $Z \propto 1/i\omega$ for the spring and $Z = cst$ for the damper, where $i = \sqrt{-1}$ is the imaginary number.

The measured impedance can be found by comparing the force produced by the piezoelectric elements with the motion of the plate. When no finger is touching the plate, the measurement reflects the dynamic behavior of the plate by itself. However, the contact with the finger modifies the dynamic behavior of the plate, leading to a shift in the phase and amplitude of the motion of the plate and a variation of the mechanical impedance of the plate. The observation of the impedance of the plate/finger system in real time such as in [15] offers the opportunity of controlling the interaction with the knowledge of its mechanical coupling. This article dives deeper in the effect that the biomechanical properties of the skin and the coupling made by the partial squeeze-film levitation have on the impedance observed via comparing the effort produced by the piezoelectric actuators and motion of the plate.

3 MODELING CONTACT DYNAMICS

The complex interaction between the finger and the vibrating plate is captured by a simple two degree of freedom model. One of the mobility is related to the motion of the skin and the other to the motion of the plate. The lumped-elements related to the soft tissues have the subscript t and the ones in relation to the behavior of the plate, the subscript p. Both parts are connected by a spring-damper element, to simulate the action of the contact and partial levitation. The subscript c refers to the contact. The model is presented in Fig.1. Two external forces are applied to this system. f_e models the action from the finger motion and subsequently captures the slow behavior of the compression of the pulp and the levitation of the skin. The other is the effort provided by the piezoelectric actuator f_a that is a single-tone harmonic excitation in the near ultrasonic range.

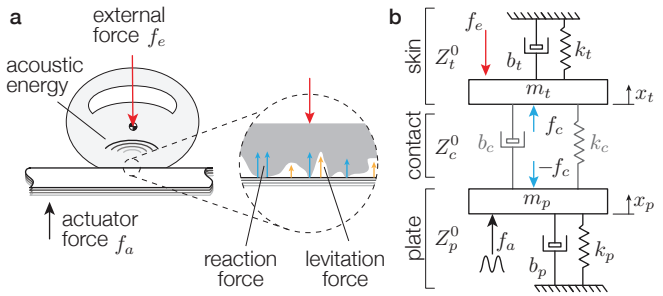

Fig. 1. **a**. Schematic of the interaction. The finger rests on the vibrating plate under external force provided by the muscle. The vibration is the consequence of a harmonic force produced by the actuator and will transfer energy to the interface (inset) and subsequently to the skin. The interaction at the small scale involves contact and partial levitation of the skin asperities. **b**. A two degree of freedom model of the interaction. Around the ultrasonic excitation frequency, both the plate and the fingertip can be modelled as second order mass-spring-damper system. The interaction from the contact and partial levitation can be lumped into a spring and damper that transmit the force between both bodies.

The force experienced by the finger will has two time-scales, one for the slow varying deformation of the pulp due to the muscular forces and the levitation and the other from the ultrasonic vibration of the plate and tissues. The system is analyzed at these two time-scale separately then combined using the superposition principle.

3.1 Constitutive equations

Analyzing the free body diagram of each mass illustrated Fig. 1 leads to the following system of equations:

$$\begin{aligned} m_t\,\ddot{x}_t \;+ b_t\,\dot{x}_t \;+ k_t\,x_t \;&=\; f_c - f_e \\ m_p\,\ddot{x}_p + b_p\,\dot{x}_p + k_p\,x_p &= -f_c + f_a \end{aligned} \tag{1}$$

where m_p, b_p, k_p stands for mass, damping and stiffness of the plate, m_t, b_t, k_t for mass, damping and stiffness of the fingertip. The connection between both mass is expressed by the exchange of force:

$$b_c\,(\dot{x}_p - \dot{x}_t) + k_c\,(x_p - x_t) = f_c \tag{2}$$

where b_c, k_c for the damping and stiffness of the partial levitation at the contact.

3.2 Harmonic behavior

The analysis starts with the harmonic behavior of the model at the excitation frequency, which is usually set around 40 kHz. Around this frequency the plate is assumed to acts as a second order system and the system of equations 1 and 2 can be transformed in the Fourier domain. The harmonic force produced by the actuator is $f_a = \hat{f}_a\, e^{i\omega t}$, where t is the time variable, $i = \sqrt{-1}$ is the imaginary number and ω is the excitation frequency set by the controller and chosen to match the resonant frequency of the plate. Since the external forces are quasi-static we can set $f_e = 0$. The respective velocities $v = \dot{x}$ of skin and the plate are $v_\beta = \hat{v}_\beta\, e^{i\omega t - i\phi_\beta}$ with $\beta = \{t, p\}$ and ϕ_β the phase of the signal with respect to the actuator force.

Taking the integral and derivative the harmonic force and displacement leads to the expression of the constitutive equations in the Fourier domain:

$$\left(m_t\,i\omega + \frac{k_t}{i\omega} + b_t\right) v_t + \left(b_c + \frac{k_c}{i\omega}\right)(v_t - v_p) = 0 \tag{3}$$

$$\left(\underbrace{m_p\,i\omega + \frac{k_p}{i\omega}}_{=0} + b_p\right) v_p + \left(b_c + \frac{k_c}{i\omega}\right)(v_p - v_t) = f_a$$

which is a single-input, multiple-outputs linear system of equations. At the resonance frequency, the inertia and stiffness of the plate cancel each other such that $k - m_p\,i\omega^2 = 0$. For generality, the reminder of the article includes these terms. This set of equation can be compactly written by expressing the impedance of each independent part taken in isolation. To denote that the impedance is computed in isolation and with no external force, we added the superscript 0. The isolated plate, tissue and contact impedance are respectively defined to:

$$Z_t^0(\omega) = \frac{\hat{f}}{\hat{v}_t} e^{i\phi_t} = m_t i\omega + \frac{k_t}{i\omega} + b_t \tag{4}$$

$$Z_p^0(\omega) = \frac{\hat{f}}{\hat{v}_p} e^{i\phi_p} = m_p i\omega + \frac{k_p}{i\omega} + b_p \tag{5}$$

$$Z_c^0(\omega) = \frac{\hat{f}}{\hat{v}_t e^{i\phi_t} - \hat{v}_p e^{i\phi_p}} = \frac{k_t}{i\omega} + b_t \tag{6}$$

Because ω is fixed, each impedance is simply a complex number. The real part of the impedance captures the energy that is absorbed and the imaginary part captures the energy reflected. Using this shorthand notation, the system of equation can be written in a matrix form:

$$\begin{pmatrix} Z_t^0 + Z_c^0 & -Z_c^0 \\ -Z_c^0 & Z_p^0 + Z_c^0 \end{pmatrix} \begin{pmatrix} v_t \\ v_p \end{pmatrix} = \begin{pmatrix} 0 \\ f_a \end{pmatrix} \tag{7}$$

From there we can invert the matrix and recognize that the impedance observed when comparing the movement of the plate with the force that is delivered by the actuators is:

$$Z_p = \frac{\hat{f}_a}{\hat{v}_p} e^{i\phi_p} = Z_p^0 + \frac{Z_t^0\, Z_c^0}{Z_t^0 + Z_c^0} \tag{8}$$

This equation show that the impedance measured at the plate is the isolated impedance of the plate associated in series with another impedance, which is the parallel association of the contact impedance and the fingertip impedance.

When the plate is completely decoupled from the finger, $Z_c^0 = 0$ the above equation gives the expected results that the impedance, observed from the vibration sensor and applied force, is equal to the isolated impedance of the plate $Z_p = Z_p^0$. Conversely, when the contact is of infinite stiffness $Z_c = \infty$, the impedance measured at the level of the plate is the impedance of the plate in series with the impedance of the contact $Z_p = Z_p^0 + Z_f^0$. This hypothesis of infinite contact stiffness is the basis of what is used in [13], [15] to find the impedance of the fingertip offline or during the interaction. Lastly, the harmonic force at the interface f_c, derived in Kaci et al. [16], can be recovered from $f_c = Z_p^0\, v_p - f_a$, where v_p and f_a are measured in real time and Z_p^0 is found when the plate is unencumbered by the finger.

3.3 Harmonic simulation

Figure 2 shows a simulation of the effect of the contact stiffness k_c on the the impedance seen by the plate and the ratio of tissue velocity to plate velocity when realistic parameters are plugged in the model. The setup considers that a typical fingertip of mass $m_t = 0.4$ g and damping 93 N.s/m is in contact with the plate. The plate natural resonant frequency is set at $f_0 = \omega\,/\,2\pi = 35$ kHz, its mass at $m_p = 17$ g, its stiffness is found to be $k_p = (2\pi f_0)^2\, m_p = 800$ N/µm. The quality factor is set at 300 leading to a damping of $b_p = \sqrt{k_p m_p}/Q = 12.4$ N.s/m. These values are representative of a vibrating plate with dimension $100 \times 22 \times 3$ mm^3.

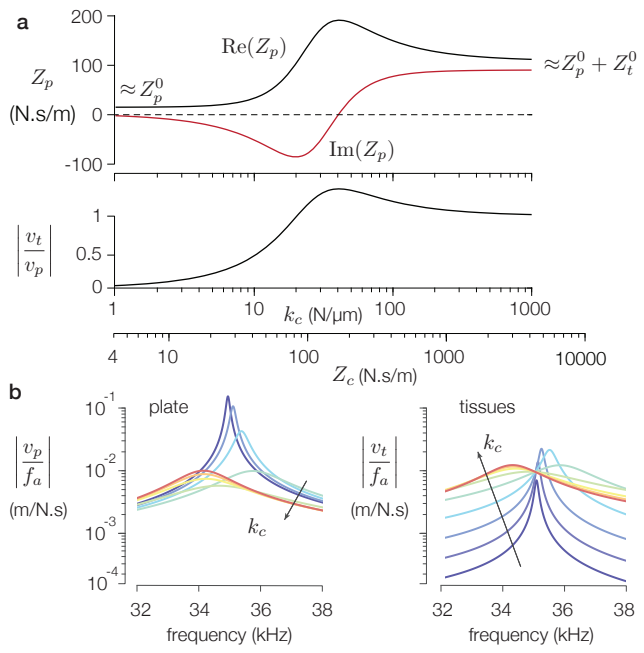

Fig. 2. **a**. Simulation of the impedance of the plate and of the relative velocity between the skin and the plate, as a function of the stiffness of the contact. Low contact stiffness decouples the skin from the glass plate, so impedance of the plate is near to its value in isolation. High contact stiffness completely couples the skin motion to the plate. **b**. Bode diagram of plate and skin movements near the resonance frequency of the plate. The increase of contact stiffness k_c is color coded.

Consequently, the velocity ratio evolve between 0 for low contact stiffness to 1 for stiff coupling. As the stiffness of the contact increases around 20, the coupling is soft enough that the impedance of the fingertip is barely reflected but high enough that the contact acts as a pure stiffness, therefore producing negative imaginary impedance. When the impedance of the contact is higher than the one from the fingertip, i.e. $k_c > 20$ N/µm, the observed impedance, mostly reflects the added mass and damping from the fingertip.

3.4 Quasi-static regime

The contact impedance, Z_c^0, is a critical factor in the dynamic behavior of the plate and fingertip system but remains to be determined. This impedance, likely to be composed of a spring and a damper, is the results of a rather complex interaction between the contact of the skin on the plate, and the acoustic force generated by the ultrasonic wave [9]. The damper, which captures the losses due to air escaping the contact, is likely to be small for this range of frequencies since the squeeze number is larger than 36 and therefore will not be studies in the reminder of the article. In order to get a better understanding of the value and how the amplitude of the plate vibration affects the stiffness of the contact, we analyze the system described in figure 1 on a slow time-scale, where the individual oscillations of the ultrasonic vibration are not captured but contributes to the quasi-static levitation. On this time-scale, $\langle f_a \rangle = 0$ and only f_e affects the behavior, therefore the force at the contact is $f_c = f_e$. This quasi-static analysis reveals that the contact impedance is non-linearly related to the amplitude of vibration.

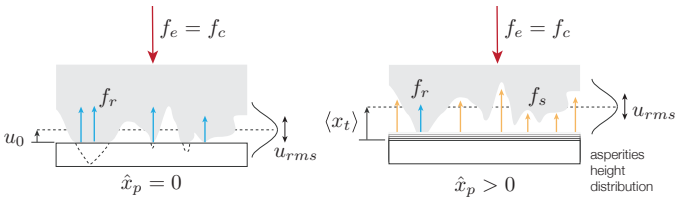

Fig. 3. Schematic of interaction between the fingertip and the ultrasonic vibrating plate. Forces from asperities in contact f_r, squeeze film levitation f_s and muscular activation f_c are balanced. On the long time-scale, the contact force f_c is only affected by external load f_e.

Following the development explained in the supplementary materials of [9], at the contact an equilibrium is found between the contact forces applied f_c, the acoustic forces from the vibration of the plate f_s and the contact force from the compression of the asperities of the skin f_r:

$$f_c = f_r + f_s \tag{9}$$

In order to follow force balance and contact parameters, an illustration of intimate contact equilibrium is provided figure 3. An approximate expression of the acoustic force can be found by deriving Reynolds lubrication equation in the gap between the finger and the plate such that:

$$f_s = \frac{5}{4} p_0\, S \frac{\hat{x}_p^2}{\langle x_t \rangle^2} \tag{10}$$

where p_0 is atmospheric pressure on its contact surface $S \approx 10$ mm^2. The amplitude of the ultrasonic vibration acting on the plate is $\hat{x}_p$ as previously defined in the harmonic analysis. Here, we set the time-average displacement of the plate to be null, i.e. $\langle x_p \rangle = 0$ so that the average gap

between both surface $\langle x_t \rangle$ is the time-average position of the finger.

In addition to the force from acoustic pressure, the fingertip is also supported by the contact made by the asperities at its surface. A relationship between the average gap and the reaction force can be found using multi-scale contact theory [29]:

$$f_r = p_c \, S \exp\left(\frac{-\langle x_t \rangle}{u_{rms}}\right) \tag{11}$$

where $p_c = 0.375 \, q_0 \, u_{rms} \; E/(1-\nu^2)$ is the pressure coefficient that captures the elasticity of the asperities. This value is affected by the roughness via u_{rms}, the elastic properties of the material via the Young's modulus E and Poisson coefficients ν, as well as the scale q_0 at which the measurement are made. See [9], [29] for more details on the derivation.

Considering the equilibrium in the absence of vibration the previous equation can be re-written as:

$$f_r = f_c \exp\left(\frac{-\langle x_t \rangle + u_0}{u_{rms}}\right) \tag{12}$$

where $u_0 = u_{rms} \ln(p_c \, S / f_c)$ is the average gap made by the contact in the absence of vibration.

Replacing 10 and 12 in the equilibrium equation 9 leads to:

$$f_c \left[1 - \exp\left(\frac{-\langle x_t \rangle + u_0}{u_{rms}}\right)\right] = \frac{5}{4} p_0 S \frac{\hat{x}_p^2}{\langle x_t \rangle^2} \tag{13}$$

This last equation can be solved numerically to find the levitation gap $\langle x_t \rangle$ as a function of the amplitude of the vibration $\hat{x}_p$. Plugging back the results leads to a force-displacement diagram representing the forces of the contact f_c and the amplitude of vibration. Figure 4 show a simulation for $u_{rms} = 5$ µm

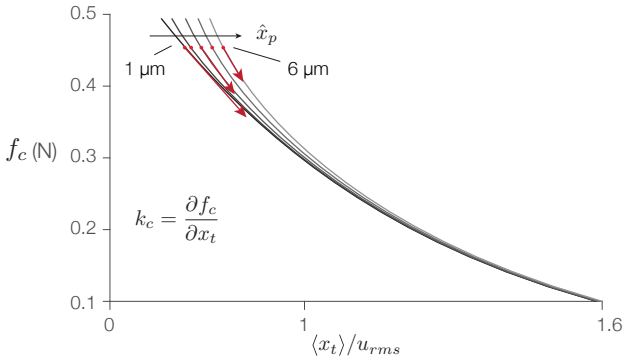

Fig. 4. Force-gap relationship at the interface for increasing amplitude of vibration. The red dots indicate the equilibrium point between the contact and acoustic pressure found for a normal force of 0.45 N. The stiffness of the contact made by undergoing partial squeeze-film levitation is computed from the gradient of this curve at the equilibrium point.

The stiffness of the contact is found by taking the partial derivative of the force over a small change of gap:

$$k_c = \frac{\partial f_c}{\partial x_t} \tag{14}$$

The effect of the vibration amplitude $\hat{x}_p$ on the levitation gap and the stiffness of the contact are shown in figure 5.

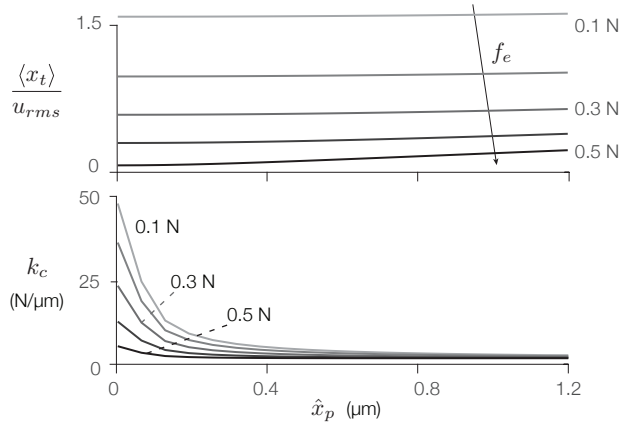

Fig. 5. Dimensionless interfacial gap $\langle x_t \rangle / u_{urms}$ and relative contact stiffness k_c function of the amplitude of vibration for a set of normal forces.

Increasing the amplitude of vibration, will lead to a larger gap, consistent with partial levitation, and a decrease of the contact stiffness. The most noteworthy fact is that every simulation of k_c asymptotically tends to 0, leading to a decoupling of the finger from the plate for sufficiently high amplitude of vibration.

3.5 Impedance as a function of vibration amplitude

The effect of fingertip contact for different amplitude of vibration on the observed impedance of the plate can be found by combining the dynamic analysis of the system with the quasi-static analysis of the contact. Fig.6 shows finger and plate impedance function of amplitude of vibration for an external force of 0.3 N.

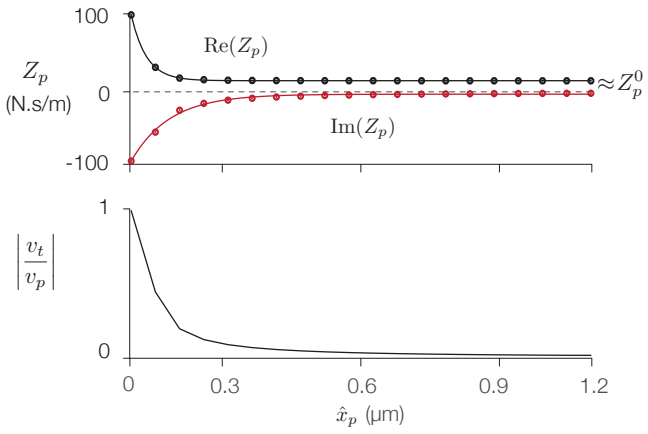

Fig. 6. **a.** Simulation of the real and imaginary parts of the plate impedance Z_p as a function of amplitude of vibration $\hat{x}_p$ for an external load of 0.3 N. Points stands for a simulation point of a defined amplitude, and lines are for the exponential fit of it from equation 15. **b.** Velocity ratio v_t/v_p function of the amplitude of vibration follows the same exponential decrease characterising real impedance decrease.

The real and imaginary part of the complex impedance of the plate and finger system, decreases exponentially with increasing amplitude and is well approximated by the

function:

$$\mathrm{Re}(Z_p(\hat{x}_p)) = \mathrm{Re}(Z_p^0) + \mathrm{Re}(Z_p^{max}) \exp(-\lambda_r \hat{x}_p)$$
$$\mathrm{Im}(Z_p(\hat{x}_p)) = \mathrm{Im}(Z_p^0) + \mathrm{Im}(Z_p^{max}) \exp(-\lambda_i \hat{x}_p) \quad (15)$$

where $Z_p^{max} = Z_p(0) - Z_p^0$ is the theoretical shift of impedance imposed by the finger when no vibrations are applied, Z_p^0 the isolated impedance of the plate and λ_r and λ_i the decay parameter for the real and imaginary part of the impedance. Using the parameter of the reference plate and of the reference finger used earlier, we found $\lambda_r \simeq 11.5$ and $\lambda_i \simeq 7.2$ for an external load of 0.3 N. The regression of the exponential function leads to a goodness of fit of $R^2 = 0.97$. λ_r and λ_i relate to the ease at which the coupling plate/finger can be reduced by increasing amplitude and points a important parameter of squeeze-film levitation efficiency. λ_r is related to the real part of the impedance Z_p and therefore the dissipation of the acoustic energy by the finger. Conversely λ_i is related to the imaginary part of Z_p and therefore to the reflection of the energy by the finger.

The model can give insight in the amount of displacement which is transferred to the skin, seen Figure 6b. For low amplitude, when the coupling is stiff, the tissues experiences motion of amplitude about the motion of the plate. As amplitude of the plate increases, the motion of the tissues is only a small fraction of the motion of the plate.

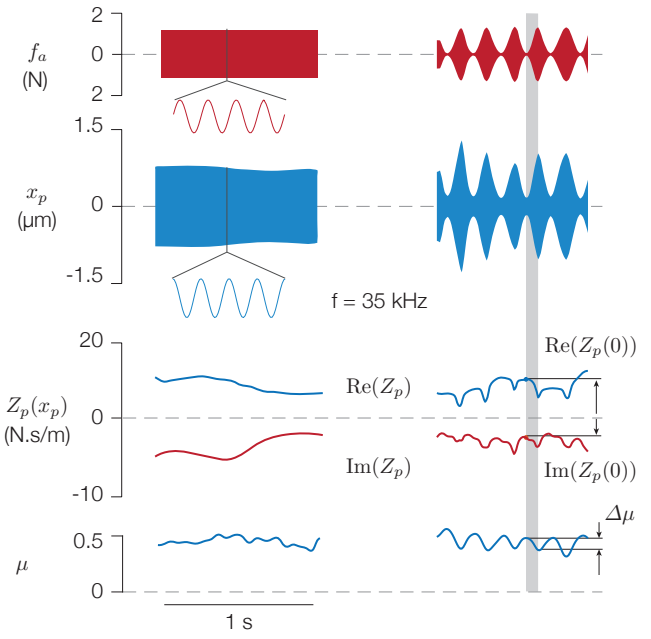

Fig. 8. Time series of the plate vibration, impedance and friction force. The set on the left is data with a constant amplitude. On the right side are data from a 4 Hz amplitude-modulated a excitation. The amplitude of vibration is the carrier frequency modulated by the envelop $\hat{x}_p$. The grey shading represents the data collection when the amplitude of the carrier rises.

4 Experimental Validation

In this section, the predictions of the model are compared to experimental data gathered during the tactile exploration of a glass plate vibrating at ultrasonic frequency.

4.1 Apparatus

The experimental studies was performed using a $105 \times 22 \times 3.3$ mm^3 borosilicate glass plate, with mass $m_p = 17$ g, stiffness $k_p = (2\pi f_0)^2 m_p = 8.2$ N/m, and Q factor is 300. The value of the damping form internal friction of $b_p = \sqrt{k_p m_p}/Q = 12.5$ N.s/m. The bode diagram of the glass plate with and without finger is presented Fig. 7. We used a function generator (B&K Precision 4052, Yorba Linda, CA, USA) to produce a carrier signal at 34917 Hz sine wave, which correspond to the natural resonant frequency of the glass plate. The modulated signal is then amplified $\times 20$ (WMA-100, Falco Systems, Katwijk, Netherlands) and fed to two piezoelectric disks glued on the glass plate. Their combine action leads to a force factor of 0.13N/V. Their deformations induce deflection of the glass plate along the 0×1 mode. the deflection of the surface is measured by a third piezo-ceramic disk acting as a sensor. The output of the piezoelectric pickup was calibrated with an interferometer (IDS 3010, Attocube, Munich, Germany) to get the glass plate vibration in micrometers. Input voltage into the piezoelectric actuators and plate vibrations were measured with an acquisition card (NI USB-6211 National Instrument) at a 100 kHz sampling rate, providing about 3 points per cycle. Lateral and normal forces imposed by the user on the plate were measured with a custom force sensor holding the glass plate [30].

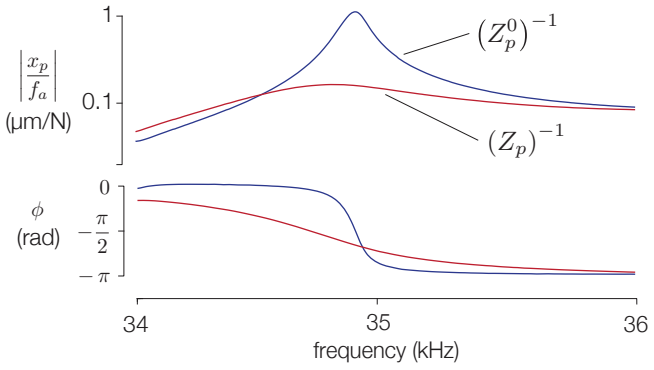

Fig. 7. Bode diagram in amplitude and phase of the glass plate used for experimental validation. The blue curve shows the frequency response of the unloaded glass plate, and the red curve shows the frequency response of the glass plate with a finger applying a constant force around 0.5N. Vibrations of the glass plate were measured during a swipe in frequency between 34 and 36 kHz.

4.2 Protocol

17 participants took part in the experiment, 5 female and 12 male, aged from 22 to 42 with a mean of 28.2 year-old. They explored the glass plate from left to right and from right to left with a constant normal force of 0.5 N and received a feedback on their regularity between each exploration. In order to ensure a consistent finger velocity across trials, subjects synchronized their movement with a moving cursor at 50 mm/s on a screen over the sliding surface and spatially correlated with its finger. From the 17 datasets, we rejected 4 because of a high normal force variability throughout the experiment (± 0.3N).

Measurement of lateral force and plate vibration amplitude for one trial is presented Fig.8. This set of data has been cut to keep only instances where the finger is fully sliding in the middle of the plate. These data are used to observe friction and impedance variability through time. Since the vibration of the plate is modified by skin contact the actual amplitude of vibration measured on the plate has a different modulation than the force applied by the piezoelectric actuators.

4.3 Mechanical impedance measurement

The mechanical impedance of the plate is found via self-sensing. The derivation of the mechanical impedance from the signals coming from the actuation and the vibration of the plate is based on the method described in the second part of [15]. For clarity, the measured variables are manifested with a superscript m in the following text.

Plate deformation $x_p^m(t)$ is first differentiated with respect to time to find velocity $v_p^m(t)$. The time-varying voltage is converted to force $f_a^m(t)$ using the force factor. The complex value harmonic motion are recovered from the real valued measurements using Hilbert transform such that:

$$v_p(t) = v_p^m(t) + i\mathcal{H}(v_p^m(t)) \qquad = \hat{v}_p\, e^{i\omega t - \phi} \tag{16}$$

$$f_a(t) = f_a^m(t) + i\mathcal{H}(f_a^m(t)) \qquad = \hat{f}_a\, e^{i\omega t} \tag{17}$$

where $\mathcal{H}(\circ)$ denotes the Hilbert transform. Once the complex value signals are recovered, the complex impedance of the plate/finger system is found via:

$$Z_p(t) = \frac{f_a(t)}{v_p(t)} \tag{18}$$

This last equation provides a real time estimate of the impedance which is showed fig.8. The isolated impedance Z_p^0, defined in section 3.2, is obtained by measuring the amplitude and phase of the motion without any load from the fingertip. Once the isolated And using equation 8, it is possible to measure the parallel association of the contact impedance with the finger impedance:

$$Z_p - Z_p^0 = \frac{Z_t^0\, Z_c^0}{Z_t^0 + Z_c^0} \tag{19}$$

4.4 Results

Figure 9a shows the coupled mechanical impedance as a function of the amplitude for a typical subject. The experimental data agree with good accuracy ($R^2 = 0.80 \pm 7$) with the exponential decay predicted by the simulation found section 3.4. Since the successive exploration are close in time, we assumed that the biomechanical behavior of the subject's fingertip was not modified significantly between them. Therefore it is possible to estimate the tissue impedance assuming that for no vibration $Z_p - Z_p^0 = Z_t^0$. Once isolated plate and tissue impedance are found, it is possible to extract the impedance of the contact at all the amplitudes of vibration from equation 19. The results of the estimation of the stiffness of the contact and the average gap, based on the exponential regression for one dataset, can be found at figure 9b and c respectively.

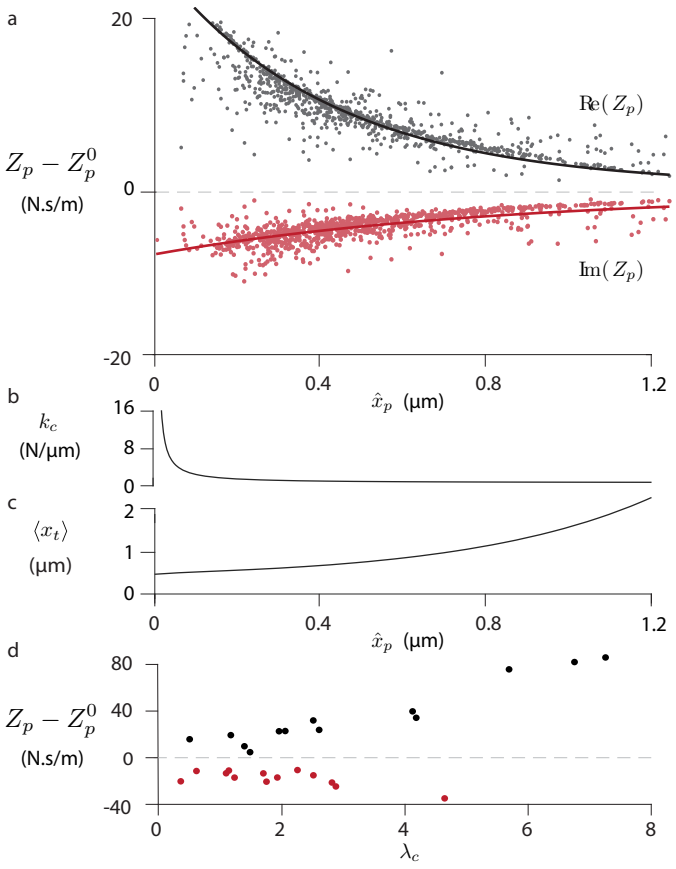

Fig. 9. **a.** Measured impedance $Z_p - Z_p^0$ added to the plate for 10 typical interactions of a sliding finger on an ultrasonic vibrating plate for one subject. Dots show the individual datum and lines the fitted exponential decay. **b.** Estimated stiffness of the contact. **c.** Estimated levitation distance of the finger. **d.** Real and imaginary part of the measured initial impedance $Z_p(0) - Z_p^0$ as a function of exponential decay parameter λ for 13 participants.

The inter-subject variability of the exponential regression of the impedance as a function of amplitude is shown Figure 9d. The decay of the exponential of the real and imaginary part λ_c is highly variable from participant to participants, with some showing almost no decay $\lambda_r = 0.1$ and other showing rapid decay $\lambda_r = 8$. This variability is likely to be caused by difference in levitation distance, with some participants having more susceptibility to levitation than others. Real part of the initial impedance $Z_p(0) - Z_p^0$ and the exponential decay λ_r has a Spearman's rank $\rho = 0.89$ revealing that low impedance skin are less susceptible to amplitude changes.

The connection between the amplitude and the observed friction force using ultrasonic friction modulation is known to be variable from trials to trials and the same is true between impedance and the coefficient of friction. Nonetheless during the observation of a single slow increase of the amplitude of the ultrasonic vibration, the correlation between the gap and the decrease of friction force can be found. Figure 10a shows the typical evolution of the the friction coefficient as a function of the average gap $\langle x_t - x_p \rangle$ during one increase of amplitude. Similarly Figure 10b reports the evolution of the frictional coefficient as a function of the estimated acoustic force, similar to [16].

The range of observed friction coefficient $\Delta\mu$, illustrated in fig.8, of each participant is compared to the the range of observed average gap $\Delta\langle x_t - x_p\rangle$ to form the scatter plot shown figure 10c. Range of friction coefficient and range of gap variation are correlated with a Sprearman's rank of $\rho = 0.82$.

Lastly the range of friction force and the range of acoustic force, shown fig.8, exhibit a positive but smaller correlation with a Spearman's rank of $\rho = 0.42$.

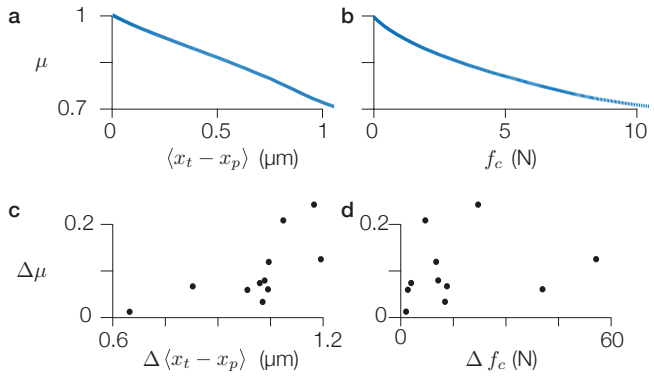

Fig. 10. **a.** Coefficient of friction as a function of the average gap for a typical trial. **b.** Coefficient of friction as a function of the amplitude of the acoustic force for a typical trial. **c.** Relation between the variation of the coefficient of friction with the variation of gap for all trials. Its Spearman's correlation rank is $\rho = 0.82$. **d.** Relation between the variation of the coefficient of friction with the variation of gap for all trials.

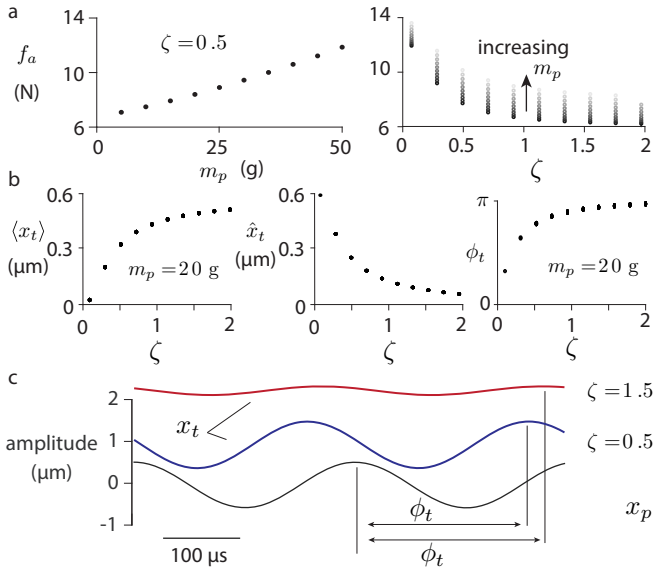

Fig. 11. **a**. Influence of glass plate mass m_p and skin damping ratio ζ on actuation force $\hat{f}_a$. **b**. Average gap $\langle x_t\rangle$ and skin position amplitude $\hat{x}_t$ and its shift ϕ_t as a function of skin damping ratio ζ. **c**. Time-domain evolution of the plate and fingertip motion for two damping ratio.

5 Parameters Influencing Impedance

The present model, supported by experimental data, is a useful means of understanding the contribution of dynamic parameters to the levitation efficiency. First, we sought to understand how the plate mass affected the dynamic properties of the system. We varied m_p, scaling the stiffness and internal damping so that the resonant frequency and the Q-factor remain constant. In addition, we studied the effects of the damping ratio $\zeta = b_f/(2\,m_f\,\omega)$ of the fingertip which is known to significantly affect the friction-modulation behavior [13].

Figure 11a shows the influence of the mass and the damping ratio on the force required by the piezoelectric actuator to sustain a vibration amplitude of $\hat{x}_p = 0.5\mu$m. The mass of the plate m_p varies from 0.5 to 50 g and the skin damping ratio ζ from 0.1 to 2. As might be expected, heavier glass has larger internal damping and therefore require larger force to reach a certain amplitude. Heavier plate masses will also give less reliable skin impedance measurements, since a greater mass increase Z_p^0 which contributes for the most part to Z_p. On the other hand, a finger with a high damping ratio requires less force to reach the prescribed motion amplitude, confirming the results from Fenton Friesen et al. [13] that over-damped tissues are more susceptible to ultrasonic friction modulation.

The damping ratio of the skin affects the levitation in many ways. First, at higher damping ratios, the energy generated by the levitation increases the gap, whereas fingers with lower damping ratios tend to oscillate more strongly, thus loosing energy to viscosity, see Figure 11b. Secondly, the damping ratio has a considerable influence on the phase between the motion of the plate and that of the skin. When the damping ratio is small, the skin behaves like a mass pushed down by external forces but continues to move synchronously with the plate, rendering levitation unlikely. Thirdly damping ratio has an influence on amplitude of skin motion. Highly damped tissues absorb energy from plate motion as a consequence skin vibration is only a small portion of plate vibration. Instantaneous gap is the distance between the plate and the fingertip at an ultrasonic timescale. So skin vibration amplitude and phase modifies this gap. Since correlation between interfacial gap and friction is exponential, not only average gap contributes to friction but also instantaneous one. In summary the results show that a fingertip with high damping ratio impacts the phase shift between the skin and the plate, which leads to larger average gap, thus reducing the motion amplitude of the skin.

Figure 11c shows the motion of the plate and of a lightly damped as well as a highly damped skin. Through its non-linear behavior, the squeeze-film levitation induces non-intuitive behavior where a high damping ratio will result, not necessarily in more viscous losses but in larger levitation distances. Larger levitation distance means that the plate is free to move almost as if the fingertip was not present, and less acoustic energy is consumed therefore.

6 Discussion

6.1 Partial squeeze-film levitation

The non-linear model of the interface between an ultrasonically vibrating plate and the fingertip, based on partial squeeze-film levitation, correctly predicts the exponential decay of the loaded plate impedance with respect to the amplitude of vibration. These results shows up the mechanical coupling behavior of the contact and vindicate the

hypothesis that the skin is levitated above the plate by the pressure resulting from the ultrasonic vibrations.

This does not mean that the skin is static, quite the contrary. The model reveals that the tissues undergo oscillatory motion, at the same frequency than the vibration of the plate. Skin motion is most prominent when, on one hand, the damping of the skin is low, as shown experimentally in [13], [22] and, on the other hand, when the amplitude of vibration is limited. In realistic conditions, i.e. where the skin has a damping ratio above 0.5, tissues oscillations are out of phase with the ultrasonic motion, which is again consistent with experimental finding [9]. The evidence suggests that the skin is bouncing on the squeeze-film of air. There is no evidence within dynamics of tissues, that skin could vibrates faster than the frequency of ultrasonic wave, suggesting that hard impacts are not likely and the interaction is smooth. The gap between the skin and the plate has a continuous sine motion during one period of the oscillation, suggesting that the contact is constant and not intermittent, and the number of asperities of the skin in intimate contact with the plate evolves at that time-scale.

For extreme amplitudes of vibration, the model asymptotically predicts a complete decoupling of the plate and skin, which in this case would mean that the levitation is total and that the skin is not in intimate contact with the plate and floats under the action of the acoustic pressure.

6.2 Levitation gap and friction reduction

In addition to the oscillatory motion of the skin, this works shows that time-average gap between the skin and the plate is strongly influenced by the amplitude and the damping of the finger. According to multi-scale contact theory, this gap is directly connected to the real area of contact made by all the skin asperities in intimate contact with the glass plate [29]. This real area of contact has been shown to be proportional to the friction coefficients for constant normal force of the skin via the shear strength of the contact [31] such that:

$$\mu \propto \exp\left(-\frac{\langle x_t - x_p \rangle}{u_{rms}}\right) \tag{20}$$

The measurement of friction force as a function of the amplitude and the estimation of the gap confirms this prediction. In addition, since a large acoustic force is required to provide a large levitation distance, the correlation between acoustic force and the friction force reported in [16], is also found. However, the robustness of the correlation of the friction coefficient with acoustic force is poorer, $\rho = 0.42$, compared to the one with the average gap $\rho = 0.82$. This is probably due to the fact that some of the acoustic force is lost through dissipation of the skin or the interface and not use toward increasing the gap and thus lowering friction. The gap on the other hand is a physical measure directly linked to the friction coefficient, which might explain its lower variability.

6.3 Self-sensing of skin biomechanics

Rendering precise and controlled stimuli on surface-haptic displays is not as direct as controlling the force output of an electromagnetic motor. Because surface-haptic displays rely on friction of the fingertip to create stimuli, the generation of the force is subject to high variability, owing to the complex tribological behavior of the skin [31] and the inherent variability in susceptibility to ultrasonic waves [15]. This work proposes to peer into the interaction that happens at the interface between the skin and the plate, by estimating the complex impedance of the tissues and of the interface itself.

Biomechanics plays an important role in the perception of the changes in friction [15], [32]. Softer or harder skin will experience more or less deformation of the tissues which has for consequence that same levels of vibration can leads to dramatic change in perception of the stimuli. A direct estimation of the impedance of the skin, which has been shown to be possible in this work when the ultrasonic amplitude is small, provide important information for shaping the input sent to the surface-haptic display and providing a consistent stimulus across users without resorting to complex force-feedback scheme [33], [34].

But more importantly, once an estimate of the skin biomechanics Z_t^0 is found, by measuring the impedance at low amplitude of stimulation, the real time measurement of the impedance of the plate can be used to probe the behavior at the interface. In fact Z_c^0 is the only unknown of equation 19. The direct measure of the impedance of the interface can allow for a real time monitoring of the levitation gap. In essence this impedance represents the coupling between the plate and the fingertip which is greatly correlated to the frictional behavior of the interface.

7 Conclusion

The amplitude of vibration of an ultrasonic plate is significantly affected by the presence of the fingertip. In this article, we modeled the dynamic and quasi-static behavior of the plate and tissues, along with a lumped-element model of the partial levitation process, including the over-pressure produced by the squeeze-film and the intimate contact of the asperities on the glass. This model allowed us to peer into the connection between the long time scale (in the order of second) capturing the relaxation of tissues and the motion impart levitation, and the ultrasonic time-scale in which we can model the diffusion and reflection of energy via a study of the plate impedance.

The main conclusion of the theoretical and experimental studies states that the higher the levitation of the skin, the less acoustic energy is used to oscillate the tissue and the more is converted toward to maintain the levitation. The model draw a clear picture of the complex interconnection between the non-linear process of squeeze film attenuation and the biomechanics of the tissues. The newfound understanding could be the basis for an improved design of the interface as well as a better control of the stimulation, not based on forces or friction coefficient, but on real-time estimation of the impedance.

References

[1] L. Winfield, J. Glassmire, J. E. Colgate, and M. Peshkin, "T-pad: Tactile pattern display through variable friction reduction," in *Second Joint EuroHaptics Conference and Symposium on Haptic Interfaces for Virtual Environment and Teleoperator Systems (WHC'07)*. IEEE, 2007, pp. 421–426.

[2] O. Bau, I. Poupyrev, A. Israr, and C. Harrison, "Teslatouch: electrovibration for touch surfaces," in *Proceedings of the 23nd annual ACM symposium on User interface software and technology*. ACM, 2010, pp. 283–292.

[3] V. Levesque, L. Oram, K. MacLean, A. Cockburn, N. D. Marchuk, D. Johnson, J. E. Colgate, and M. A. Peshkin, "Enhancing physicality in touch interaction with programmable friction," in *Proceedings of the SIGCHI Conference on Human Factors in Computing Systems*. ACM, 2011, pp. 2481–2490.

[4] G. Casiez, N. Roussel, R. Vanbelleghem, and F. Giraud, "Surfpad: riding towards targets on a squeeze film effect," in *Proceedings of the SIGCHI Conference on Human Factors in Computing Systems*. ACM, 2011, pp. 2491–2500.

[5] M. Amberg, F. Giraud, B. Semail, P. Olivo, G. Casiez, and N. Roussel, "Stimtac: a tactile input device with programmable friction," in *Proceedings of the 24th annual ACM symposium adjunct on User interface software and technology*. ACM, 2011, pp. 7–8.

[6] C. Bernard, J. Monnoyer, and M. Wiertlewski, "Harmonious textures: the perceptual dimensions of synthetic sinusoidal gratings," in *International Conference on Human Haptic Sensing and Touch Enabled Computer Applications*. Springer, 2018, pp. 685–695.

[7] M. K. Saleem, C. Yilmaz, and C. Basdogan, "Psychophysical evaluation of change in friction on an ultrasonically-actuated touchscreen," *IEEE transactions on haptics*, 2019.

[8] T. Watanabe and S. Fukui, "A method for controlling tactile sensation of surface roughness using ultrasonic vibration," in *Proceedings of 1995 IEEE International Conference on Robotics and Automation*, vol. 1. IEEE, 1995, pp. 1134–1139.

[9] M. Wiertlewski, R. F. Friesen, and J. E. Colgate, "Partial squeeze film levitation modulates fingertip friction," *Proceedings of the national academy of sciences*, vol. 113, no. 33, pp. 9210–9215, 2016.

[10] M. Biet, F. Giraud, and B. Lemaire-Semail, "Squeeze film effect for the design of an ultrasonic tactile plate," *IEEE transactions on ultrasonics, ferroelectrics, and frequency control*, vol. 54, no. 12, pp. 2678–2688, 2007.

[11] R. F. Friesen, M. Wiertlewski, M. A. Peshkin, and J. E. Colgate, "The contribution of air to ultrasonic friction reduction," in *2017 IEEE World Haptics Conference (WHC)*. IEEE, 2017, pp. 517–522.

[12] D. Ilssar and I. Bucher, "The effect of acoustically levitated objects on the dynamics of ultrasonic actuators," *Journal of Applied Physics*, vol. 121, no. 11, p. 114504, 2017.

[13] R. F. Friesen, M. Wiertlewski, and J. E. Colgate, "The role of damping in ultrasonic friction reduction," in *2016 IEEE Haptics Symposium (HAPTICS)*. IEEE, 2016, pp. 167–172.

[14] J. Monnoyer, E. Diaz, C. Bourdin, and M. Wiertlewski, "Optimal skin impedance promotes perception of ultrasonic switches," in *2017 IEEE World Haptics Conference (WHC)*. IEEE, 2017, pp. 130–135.

[15] ——, "Perception of ultrasonic switches involves large discontinuity of the mechanical impedance," *IEEE transactions on haptics*, vol. 11, no. 4, pp. 579–589, 2018.

[16] A. Kaci, A. Torres, F. Giraud, C. Giraud-Audine, M. Amberg, and B. Lemaire-Semail, "Fundamental acoustical finger force calculation for out-of-plane ultrasonic vibration and its correlation with friction reduction," in *2019 IEEE World Haptics Conference (WHC)*. IEEE, 2019, pp. 413–418.

[17] M. Wiertlewski and J. E. Colgate, "Power optimization of ultrasonic friction-modulation tactile interfaces," *IEEE transactions on haptics*, vol. 8, no. 1, pp. 43–53, 2014.

[18] E. Salbu, "Compressible squeeze films and squeeze bearings," *Journal of Basic Engineering*, vol. 86, no. 2, pp. 355–364, 1964.

[19] L. Winfield, J. Colgate, M. Lin, and M. Otaduy, "Variable friction haptic displays," *Haptic rendering: Foundations, algorithms and applications, MC Lin and M. Otaduy, Eds. AK Peters, Ltd*, 2008.

[20] E. Vezzoli, Z. Vidrih, V. Giamundo, B. Lemaire-Semail, F. Giraud, T. Rodic, D. Peric, and M. Adams, "Friction reduction through ultrasonic vibration part 1: Modelling intermittent contact," *IEEE transactions on haptics*, vol. 10, no. 2, pp. 196–207, 2017.

[21] W. B. Messaoud, E. Vezzoli, F. Giraud, and B. Lemaire-Semail, "Pressure dependence of friction modulation in ultrasonic devices," in *Work-in-Progress in World Haptics Conference (WHC)*, 2015.

[22] R. F. Friesen, M. Wiertlewski, M. A. Peshkin, and J. E. Colgate, "Bioinspired artificial fingertips that exhibit friction reduction when subjected to transverse ultrasonic vibrations," in *2015 IEEE World Haptics Conference (WHC)*. IEEE, 2015, pp. 208–213.

[23] C. Jamison, R. Marangoni, and A. Glaser, "Viscoelastic properties of soft tissue by discrete model characterization," *Journal of Biomechanics*, vol. 1, no. 1, pp. 33–46, 1968.

[24] D. L. Jindrich, Y. Zhou, T. Becker, and J. T. Dennerlein, "Non-linear viscoelastic models predict fingertip pulp force-displacement characteristics during voluntary tapping," *Journal of biomechanics*, vol. 36, no. 4, pp. 497–503, 2003.

[25] T. A. Kern and R. Werthschützky, "Studies of the mechanical impedance of the index finger in multiple dimensions," in *International Conference on Human Haptic Sensing and Touch Enabled Computer Applications*. Springer, 2008, pp. 175–180.

[26] M. Wiertlewski and V. Hayward, "Mechanical behavior of the fingertip in the range of frequencies and displacements relevant to touch," *Journal of biomechanics*, vol. 45, no. 11, pp. 1869–1874, 2012.

[27] F. Giraud, T. Hara, C. Giraud-Audine, M. Amberg, B. Lemaire-Semail, and M. Takasaki, "Evaluation of a friction reduction based haptic surface at high frequency," in *2018 IEEE Haptics Symposium (HAPTICS)*. IEEE, 2018, pp. 210–215.

[28] J. Greenwood and J. P. Williamson, "Contact of nominally flat surfaces," *Proceedings of the royal society of London. Series A. Mathematical and physical sciences*, vol. 295, no. 1442, pp. 300–319, 1966.

[29] B. Persson, "Relation between interfacial separation and load: a general theory of contact mechanics," *Physical review letters*, vol. 99, no. 12, p. 125502, 2007.

[30] C. Bernard, J. Monnoyer, S. Ystad, and M. Wiertlewski, "Interferometric tribometer for wide-range/high-bandwidth measurement of tactile force interaction," in *Work-in-Progress in World Haptics Conference (WHC)*, 2019.

[31] S. M. Pasumarty, S. A. Johnson, S. A. Watson, and M. J. Adams, "Friction of the human finger pad: influence of moisture, occlusion and velocity," *Tribology Letters*, vol. 44, no. 2, p. 117, 2011.

[32] W. B. Messaoud, M.-A. Bueno, and B. Lemaire-Semail, "Relation between human perceived friction and finger friction characteristics," *Tribology International*, vol. 98, pp. 261–269, 2016.

[33] W. B. Messaoud, M. Amberg, B. Lemaire-Semail, F. Giraud, and M.-A. Bueno, "High fidelity closed loop controlled friction in smarttac tactile stimulator," in *2015 17th European Conference on Power Electronics and Applications (EPE'15 ECCE-Europe)*. IEEE, 2015, pp. 1–9.

[34] N. Huloux, J. Monnoyer, M. Boyron, and M. Wiertlewski, "Overcoming the variability of fingertip friction with surface-haptic force-feedback," in *International Conference on Human Haptic Sensing and Touch Enabled Computer Applications*. Springer, 2018, pp. 326–337.